Urine-Powered Wireless Urinary Tract Infection Monitoring Sensor for Smart Diaper Platform

Annual Report

(August 2016 ~ July 2017)

Project Sponsored by

Catalyst Foundation

Principal Investigators

Byunghoo Jung

Babak Ziaie

Ph.D. Graduate Research Assistant

Weeseong Seo

School of Electrical and Computer Engineering

Purdue University

Summary

The goal of the project is to develop a diaper-embedded urine-activated/powered wireless sensor module for autonomously screening urinary track infections (UTI), and improve the quality of life of elderly, young children, infants, and those suffering from neurodegenerative diseases such as dementia. The specific aims for the goal are: 1) develop a colorimetric sensing mechanism for detecting nitrites in urine, 2) low-power sensing circuitry compatible with the developed colorimetric sensing mechanism, 3) power efficient wireless transmission of the sensing data, 4) urine-activated and -powered battery including regulator and DC-DC converter, 5) integrating of all components on a low-cost flexible paper substrate, and 6) providing a better accuracy compared with conventional dipstick testing.

In the first year, we developed the first version of a urinary tract infection (UTI) sensing system consisting of a custom designed urine-powered battery, an optical colorimetric UTI sensor, low power sensor interface circuits, a Bluetooth module, and an Android app displaying the sensing results. The circuits that include a DC-DC converter, an LED driver, a photo-diode interface, and a pulse width modulator, are optimized for low power consumption. An algorithm that can compensate process variations has been developed and implemented into an Android app that calculates and displays the final sensing results.

In the second year, we presented the results of the first year work at *the 2015 IEEE Biomedical Circuits and Systems (BioCAS) Conference*. The work also has been invited to *the 2016 International Conference of the IEEE Engineering in Medicine and Biology Society*. The first prototype developed during the first year has four separate modules connected through wires: a battery module, a sensor module, a sensor interface circuit module, and a Bluetooth communication module. During the second year, we reduced the number of modules to two: (a) a disposable module consisting of a urine-powered battery, a sensing unit, and a sensor interface circuit, and (b) a reusable Bluetooth communication module. Only the low-cost disposable module will be embedded into a diaper. The sensor interface design has been further optimized for improving power efficiency, and the battery has been redesigned to improve its flexibility, so it can be easily embedded in a diaper without causing any irritation.

In the third year, a part of the second year results was published on *the IEEE Transactions on Biomedical Circuits and Systems*. The latest prototype developed during the third year includes a urine-powered battery with an improved urine-absorbing efficiency, a revised colorimetric UTI sensor with an improved sensing efficiency, a firmware utilizing new time-gating protocols that improve power efficiency by more than 50%, and an Android application SW that shows the progress of the UTI sensing at real-time. To further reduce the size and improve the power efficiency of the sensing system, we are developing a custom integrated circuit (IC) that includes a DC-DC converter and regulator, an LED driver, and a sensor interface in TSMC 65nm technology. Because the power efficiency of the DC-DC converter is crucial for improving the overall system power efficiency, we developed a new DC-DC converter with a power efficiency of 88% and an output voltage ripple of 9mV over a wide input voltage range. The custom IC design has been completed and sent to TSMC for fabrication. The fabricated IC will be delivered in October 2017.

In the following year, we will characterize the performances of the fabricated custom IC, and build a new prototype UTI sensing system utilizing the custom IC. We expect significantly improvements in size and power efficiency. We will also conduct tests with natural human urine, instead of using synthetic urine, in collaboration with a urologist at the Indiana University Medical School.

[Publications]

1) Weeseong Seo, Wuyang Yu, Tianlin Tan, Jiawei Zhou, Tianshuo Zhang, Babak Ziaie, Byunghoo Jung, "Diaper-embedded urinary tract infection monitoring system powered by a urine-powered battery," *IEEE Biomedical Circuits and Systems Conference (BioCAS)*, May 2015.

2) (Invited) Wuyang Yu, Weeseong Seo, Byunghoo Jung, and Babak Ziaie, "A Diaper-embedded disposable Nitrite sensor with integrated on-board urine-activated battery for UTI sensing," *Int. Conf. of the IEEE Engineering in Medicine and Biology Society*, Aug. 2016.

3) Weeseong Seo, Wuyang Yu, Tianlin Tan, Babak Ziaie, and Byunghoo Jung, "A diaper-embedded urinary track infection monitoring sensor module powered by urine-activated batteries," *IEEE Tran. Biomedical Circuits and Systems*, vol. 3, pp. 681-691, June 2017.

I. Introduction

Urinary tract infection (UTI) is the second most common infection caused by bacterial pathogens, accounting for about 8.1 million hospital visits to health care providers in the US annually. UTI is predominantly bacterial with coliform bacteria, in particular Escherichia coli (E.coli), being responsible for most cases. It is also the most prevalent infection in the residents of long-term-care facilities with 15~50% of the cases being asymptomatic. In general, UTI is considered to be easily treatable using antibiotics. However, if not found and treated early, UTI can be a major source of serious complications such as ascending infections, loss of kidney function, bacteremia, and sepsis in infants and geriatric patients suffering from neurodegenerative diseases such as dementia. Both groups who use diapers have difficulties in communicating about urinary discomfort and UTI-associated symptoms to their care givers. These difficulties and the fact that UTI is often asymptomatic make early stage identification quite challenging.

Urine culture test is the most conventional UTI diagnose. One significant disadvantage of the current microbiology method is a lapse of 2 to 3 days between specimen collection and final diagnose. As a result, dipsticks have been widely used for less accurate but quick detection of UTIs. However, in addition to potential privacy issues, collecting urine samples from infants and disabled elderly for dipstick test is not trivial. In this regard, a better method for early detection and screening of UTIs that can alert caregivers with minimal efforts is being sought after.

Several detection systems for UTI have been presented in the literature. In one way, the same chemical factors existing in a UTI dipstick is printed on a commercial diaper with a hand-held printer which is designed to guarantee that a specific chemical factor will be printed in a specific square area. After the reaction between the chemicals and urine occurs, a camera of a smart phone records the change in colors, processes the images with a mobile application software which is designed for smartphone using technology of imaging analysis, and takes further action concerning UTI. Although this approach provides a fast detection by eliminating the time to collect urine samples, it does not offer a quantitative analysis and, more importantly, still requires an additional process to record the change in colors and process the images, prohibiting an autonomous operation. It also suffers from color fading issues because the time gap between urination and photo events is often unpredictable and the color of the sensing part fades over time when it dries up. Another issue is the contamination by stool that prohibits photo-based analysis. In another way, a mutual-capacitance measurement is used to detect the presence of E.coli using a capacitance touch screen (CTS) with surface-electrodes modified to have E.coli receptors. In the case of CTS, the errors resulted from process variations such as the capacitance variation in the CTS and the offset variation in the charge amplifier need to be compensated. Moreover, the CTS method is not autonomous because a caregiver should place the urine sample on the CTS surface manually.

We investigated a diaper-embedded, wireless, self-powered, and autonomous UTI monitoring sensor module that allows an early detection and screening of UTI with minimal effort. Fig. 1 shows a conceptual diagram representing the sensor module and system. As UTI dipsticks detect the level of nitrite, a surrogate of UTI, the sensor module quantitatively evaluates the concentration of nitrite in the urine, and transmits the information via a Bluetooth low energy (BLE) module to a nearby BLE capable mobile device. The sensor module utilizes a flexible substrate that can either be embedded in a diaper during the manufacturing process or attached as an added unit to a commercially available diaper. It is highly desirable that the disposable sensor module embedded in a diaper is self-powered because of cost and environmental issues. For this reason, the system utilized a urine-activated battery, which allows self-powered autonomous operations. Because of the limited amount of energy that the urine-activated battery provides, a power efficient yet accurate sensor interface circuit is crucial for successful operation.

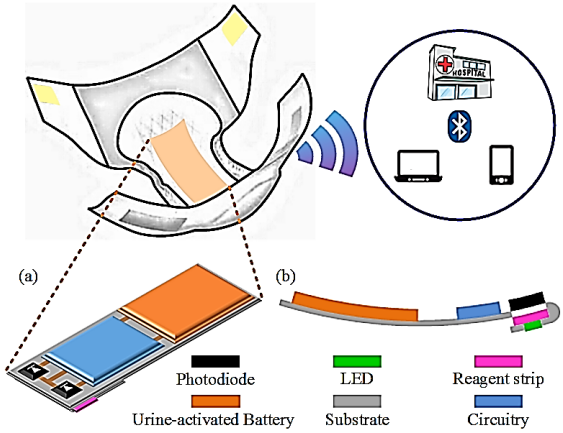

Fig. 1. Diaper-embedded UTI monitoring sensor module
(a) Diagonal view (b) Cross-section view

II. Review of the principle and design

2.1 System architecture

As shown in Fig. 2, the diaper-embedded UTI monitoring sensor module consists of a paper-based colorimetric nitrite sensor, urine-activated batteries, a boost DC-DC converter, a low-power sensor interface utilizing pulse width modulation, and a BLE module for wireless transmission. Once the urine reaches the batteries, they are activated and start to provide power to the rest of the sensor module, hence waking up the whole sensor module. This urination-event driven automatic wakeup eliminates the need for periodic wakeup for checking urination-event, which is required for a system that relies on a continuously powered battery. The output voltage of the urine-activated battery ranges from 0.3V to 0.9V, and the boost DC-DC converter increases the voltage to a regulated voltage of 2.0V. The level of power provided by the urine-powered battery varies from 3mW to 9mW, and the power conversion efficiency of the DC-DC converter falls in the range from 50% to 60%. Then, the boosted voltage powers up the colorimetric nitrite sensor, the sensor interface, and the BLE module. When the urine-absorbing strip absorbs the urine, the color of the strip changes from white to pink. The color density of the strip is proportional to the nitrite concentration in the urine and affects the amount of the light that reaches the photodiode, and consequently determines its photocurrent. The sensor interface converts the photocurrent into a pulse width modulated (PWM) signal. The BLE module has a built-in counter operating at 40kHz which transforms the PWM signal into a digital signal. This architecture utilizing pulse-width-to-digital conversion eliminates the need for an ADC, which significantly improves the power efficiency and reduces the complexity of the system. The BLE module transmits the data to a nearby BLE capable mobile device of a caregiver, which is presumably connected to a healthcare network.

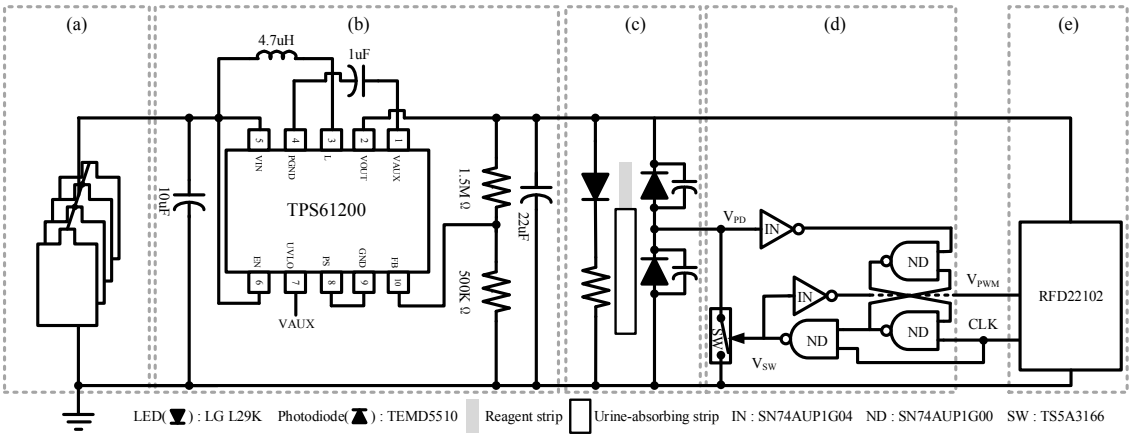

Fig. 2. A block diagram of the diaper-embedded UTI monitoring sensor module
(a) Urine-activated batteries (b) Boost DC-DC converter (c) Colorimetric nitrite sensor (d) Sensor interface (e) BLE module

2.2 Urine-activated Battery

The battery is a Zn-Cu electrochemical cell providing a theoretical potential difference of 1.1V. It is comprised of two half cells (Cu/CuSO4 and Zn/ZnCl2) and a salt bridge. The fabrication process starts with a laser machining a sheet of wax paper into a 3cm square substrate. Then, copper and zinc (50 and 100µm thick, respectively) tapes with an adhesive backing are carved into 2.5cm squares with electrical connection protrusions by the 1.06µm fiber laser to create the metal electrodes. Using the CO2 laser, filter papers impregnated with CuSO4 are shaped into corresponding squares as electrolytes overlap the copper electrodes while those with KCl are patterned as salt-bridges as well as the electrolytes for the zinc electrodes. Afterwards, a polyimide tape is also machined by the CO2 laser. Additionally, small openings are laser cut on polyimide tape and Zn tape as access holes for urine activation of the battery. In the end, the battery is assembled through aligning and taping these patterned layers and the packaging is strengthened by high temperature lamination. Fig. 3 illustrates the fabrication process. When urine wets the filter papers through the predefined openings, the redox reaction starts to take place via the moist salt bridge connecting both half-cells, supplying power to the system.

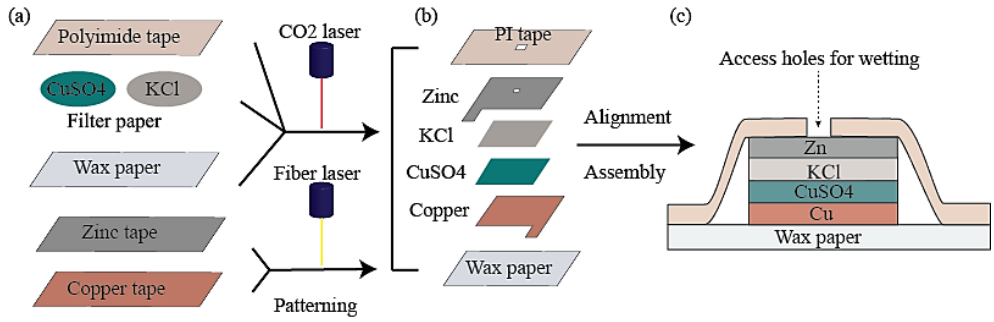

Fig. 3. Fabrication process of the urine-activated battery
(a) Laser-defining of the substrate, the active materials and the covering polyimide tape for the battery (b) Alignment and assembly of the battery (c) Schematic structure of the battery

2.3 Colorimetric Nitrite Sensor

Fig. 4 shows the structure of the colorimetric nitrite sensor. All components are integrated onto a wax paper with great expansibility and high flexibility. In order to overlap and align the LED and the active photodiode, the sensor is folded along the dashed line in Fig. 4(a), and a urine-absorbing strip and a reagent strip are placed between the LED and the active photodiode. The urine goes through the holes, reaches the urine-absorbing strip of the second layer, and then spreads until it arrives at the reagent strip of the third layer containing the "Griess reagent". The urine reacts with p-arsanilic acid to produce a diazonium compound and to couple with N-ethylenediamine dihydrochloride in order. After the reaction chains for the detection of nitrite in acid medium, the color of the reagent strip changes from white to pink. The color density reflects the concentration of the nitrite in the urine and affects the amount of the light arriving at the active photodiode after passing through the reagent strip and consequently determines the photocurrent that the active photodiode generates. The concentration of nitrite, which indicates the level of UTI, can be quantified with the amount of the active photodiode current.

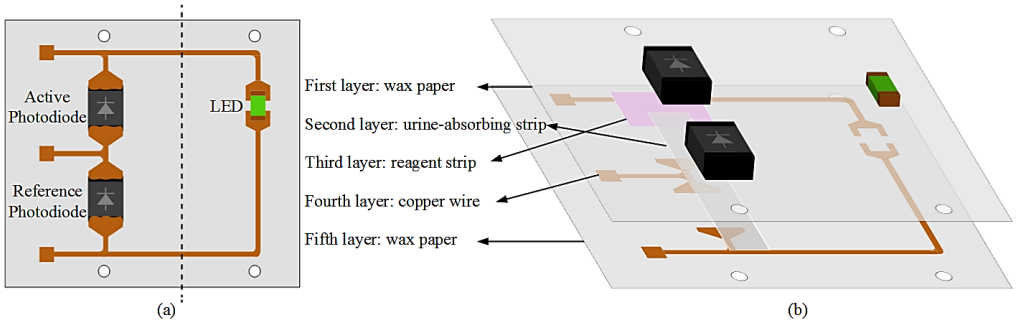

Fig. 4. (a) Colorimetric sensor on a flexible substrate (top view) (b) Exploded view of the sensor

2.4 Sensor interface with pulse width modulation

In the colorimetric nitrite sensor, the intensity of the light reaching the photodiode after passing through the urine-absorbing strip carries the information of the nitrite concentration in the urine, indicating the level of UTIs. To interpret the light intensity signal into electrical signal, typically a transimpedance amplifier (TIA) is used to turn the photodiode current into voltage, which is further encoded into digital data by an analog-to-digital converter (ADC). This conventional method increases the complexity and the power consumption of the interface circuit. Due to the limited amount of energy available from the urine-powered battery, a power efficient sensor interface is highly desirable for reliable and self-powered operation of the sensor module. To address these issues, we developed a semi-digital PWM-based method in this work, where the pulse width of the binary output signal is inversely proportional to the photodiode current, and a counter translates the pulse width into digital information. This PWM-based method allows to eliminate the complex and potentially power-intensive TIA and ADC. It also provides a wide dynamic range because the data is represented in the time domain as the pulse width rather than the voltage or current domain where its dynamic range is typically limited by the supply voltage.

Fig. 5 shows a block diagram of the two photodiodes in the colorimetric sensor and the sensor interface circuit. The sensor interface consists of two inverters, three NAND gates, and one analog switch. Two parasitic capacitors, C1 and C2, connected in parallel with the two photodiodes act as a charging capacitor.

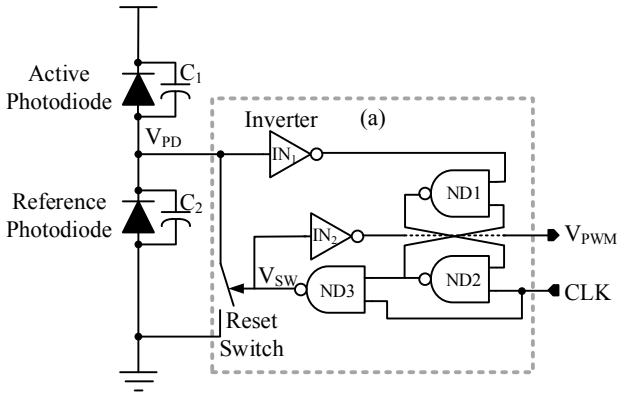

Fig. 5. The block diagram of photodiodes and sensor interface configuration.
(a) Sensor interface circuit

Fig. 6 shows the signal response of the sensor interface operation at different stages. First, the active-high V_{SW} signal changes from HIGH to LOW at the rising edge of the CLK signal coming from the BLE module and turns the Reset switch off. Then, the photocurrent (I_{PD}) initiates the charging of the node V_{PD} located between the two photodiodes and the V_{PD} signal begins to increase. Once the V_{PD} signal reaches the inverter IN_1 threshold voltage, V_{TH}, which is a fraction of the supply voltage, say αVDD, where α is a constant smaller than 1 and should be calibrated for a reliable operation due to process variations, the IN_1 output pushes the V_{SW} signal to HIGH, resetting the V_{PD} signal to the ground. The V_{PWM} signal is the inverse of the V_{SW} signal.

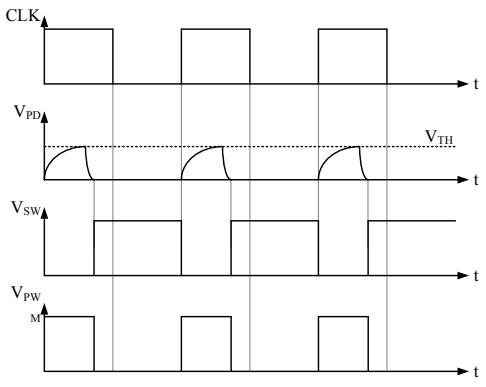

Fig. 6. Timing diagram for the sensor interface.

If we assume that the parasitic capacitances are constant during the charging with the photocurrent I_{PD}, it is simple to analyze the relation between the pulse width T_{PW} of the V_{PWM} signal and the photocurrent I_{PD} as

$$T_{PW} = \frac{(C_1 + C_2) \times \alpha VDD}{I_{PD}}$$

The parasitic capacitances, however, vary significantly during the charging process due to the dependency on its reverse bias voltage as illustrated in Fig. 7.

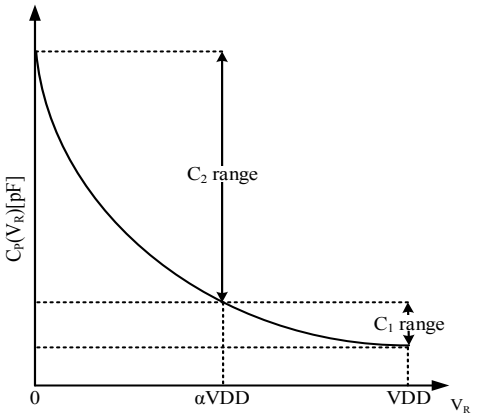

Fig. 7. Parasitic capacitance of a photodiode versus reverse bias voltage.

To obtain the pulse width T_{PW} with voltage dependent capacitors, we use an abrupt pn-junction capacitance model and express the parasitic capacitance C_P dependent on the reverse bias voltage as follows:

$$C_P(V_R) = \frac{\varepsilon_{SI}\varepsilon_0 A}{\sqrt{2\varepsilon_{SI}\varepsilon_0 A\mu\rho(V_R + \phi_{bi})}} = \frac{K_0}{\sqrt{V_R + \phi_{bi}}}, \quad \left(K_0 = \frac{\varepsilon_{SI}\varepsilon_0 A}{\sqrt{2\varepsilon_{SI}\varepsilon_0 A\mu\rho}}\right)$$

where ε_{SI} is the silicon dielectric constant, ε_0 is the permittivity of free space, μ is the mobility of the electrons, ρ is the resistivity of the silicon, V_R is the applied reverse bias voltage, is the built-in junction voltage, and A is the diffused area of the junction.

Fig. 8 shows the circuit model of the two variable parasitic capacitors.

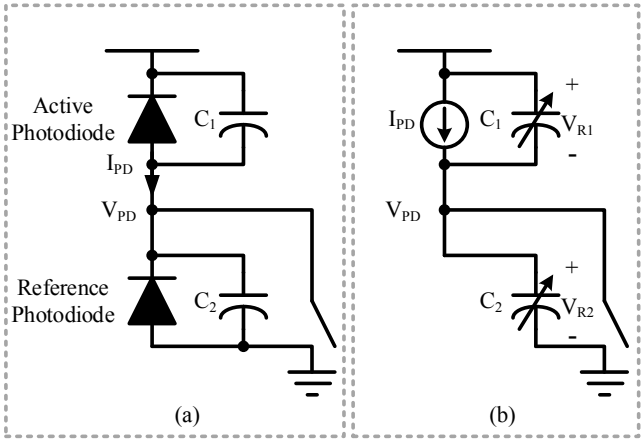

Fig.8. (a) Active and reference photodiode with parasitic capacitors C1 and C2 (b) Circuit model with the voltage dependent parasitic capacitors.

To calculate T_{PW}, we add the contributions of each parasitic capacitor of the two photodiodes. From Fig. 8(b), the parasitic capacitance C_1 of the active photodiode can be described as

$$C_1(V_{R1}) = C_p(VDD - V_{PD})$$

where $V_{R1}=VDD-V_{PD}$. In addition, the parasitic capacitance C_2 of the reference photodiode can be given as

$$C_2(V_{R2}) = C_P(V_{PD})$$

where $V_{R2}=V_{PD}$. Using (3) and (4), we can get

$$I_{PD} = \left[C_P(VDD - V_{PD}) + C_P(V_{PD})\right]\frac{dV_{PD}}{dt}$$

Performing an integral, we can describe the relation between the pulse width T_{PW} and the photocurrent I_{PD} as follows:

$$T_{PW} = \frac{1}{I_{PD}}\int_0^{\alpha VDD}\left[C_P(VDD - V_{PD}) + C_P(V_{PD})\right]\cdot dV_{PD} = \frac{\beta}{I_{PD}}$$

$$\beta = 2K_0\cdot\left(\sqrt{VDD+\phi_{bi}} - \sqrt{(1-\alpha)VDD+\phi_{bi}} + \sqrt{\alpha VDD+\phi_{bi}} - \sqrt{\phi_{bi}}\right)$$

2.5 Calibration for process variation

There exists a significant level of process variations in the LED, photodiodes, and the urine-absorbing strip. The large variation brought by the consisting elements would make a reliable operation of the sensor module almost impossible, so an effective on-line calibration method is essential.

We note that the process variations would impact the output pulse width for the dry reagent strip (before reacting with urine) and for the wet reagent strip (after reacting with urine) in the same manner. Consequently, the differential reading between the pulse width (T_{PW1}) for the dry reagent strip and the pulse width (T_{PW2}) for the wet reagent strip would suffer significantly less from process variations. To measure the difference, we use a time lapse reading technique. The sensor module is designed in such a way that the urine reaches the urine-activated batteries first, and the reagent strip later. As soon as the urine-activated batteries become active, the sensor module measures T_{PW1} while the reagent strip is dry. The following readings use T_{PW1} as a reference, and the sensor module registers the differential pulse width, $T_{DPW} = T_{PW1} - T_{PW2}$, rather than T_{PW1}. Although the effect of process variations can be partially mitigated by this time-lapse based differential reading technique, the sensor module is still vulnerable to process variations, requiring further calibrations. The proposed on-line calibration finds a process variation constant number K_{CAL} using a known reference and corrects the measured differential pulse width by multiplying the constant K_{CAL}. In this method, we use one arbitrarily selected sensor module as a known universal reference. An end-user sensor module has the performance deviation from the reference module and shows a different output pulse width at the same nitrite concentration. The measured differential pulse width of an end-user sensor module can be annotated back to the differential pulse width of the reference module by multiplying the constant K_{CAL}, as shown in Fig. 9.

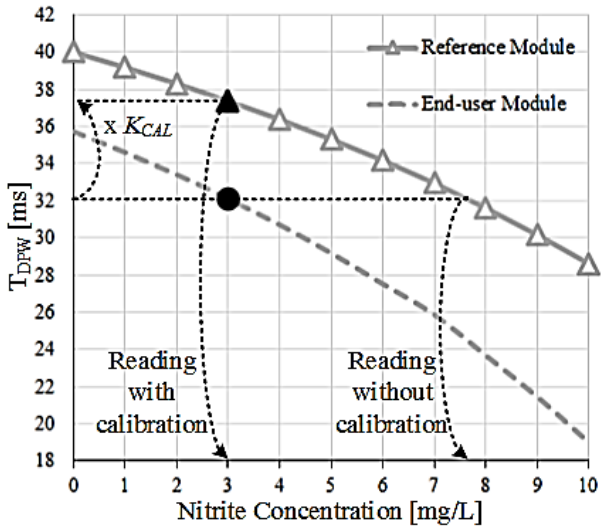

Fig. 9. Calibration for process variations.

First, we measure the nitrite concentration versus the differential pulse width curve using the known reference module as shown in Fig. 9. We can express the reference pulse widths ($T_{DPW,REF}$) by visiting the familiar formula (6) and using the differential reading technique

$$T_{DPW,REF} = \beta_{REF}\left(\frac{1}{I_{DRY,REF}} - \frac{1}{I_{WET,REF}}\right)$$

where $I_{DRY,REF}$ is a reference photocurrent when the reagent strip is dry and $I_{WET,\ REF}$ is a reference photocurrent when the reagent strip is wet. The data for the reference module is stored in the mobile device that performs the calibration operation. Because each end-user module has a different constant β, each sensor module should be able to find its own value of β unless the constant value is measured for each module during the production stage, which is challenging because the module is intended for one-time use and to be disposable. In the developed system, each sensor module finds the value of β autonomously utilizing the dry condition measurement. For the time lapse based differential measurement, the sensor module first measures the pulse width T_{PW1}. Because the nitrite concentration in the urine should not affect the constant β, we can calculate the constant K_{CAL} using the measured T_{PW1} and the known value of $T_{PW1,REF}$ from the known reference.

$$K_{CAL} = \frac{T_{PW1,REF}}{T_{PW1}} = \frac{\beta_{REF}}{\beta} \cdot \frac{I_{DRY}}{I_{DRY,REF}}$$

As the process variations would impact the output pulse width for the dry reagent strip and for the wet reagent strip in the same manner, we can express the relationship between the two reference currents and the two end-user currents as

$$I_{DRY} = \varepsilon I_{DRY,REF},\ I_{WET} = \varepsilon I_{WET,REF}$$

where I_{DRY} is an end-user photocurrent when the reagent strip is dry and I_{WET} is an end-user photocurrent when the reagent strip is wet. The calibrated differential pulse width $T_{DPW,CAL}$ can be obtained by multiplying the calculated constant K_{CAL} to the measured differential pulse width:

$$T_{DPW} = \beta\left(\frac{1}{I_{DRY}} - \frac{1}{I_{WET}}\right)$$

$$T_{DPW,CAL} = K_{CAL} \cdot T_{DPW} = \beta_{REF}\left(\frac{1}{I_{DRY,REF}} - \frac{I_{DRY}}{I_{DRY,REF}}\frac{1}{I_{WET}}\right)$$

$$= \beta_{REF}\left(\frac{1}{I_{DRY,REF}} - \frac{1}{I_{WET,REF}}\right)$$

III. Experimental results

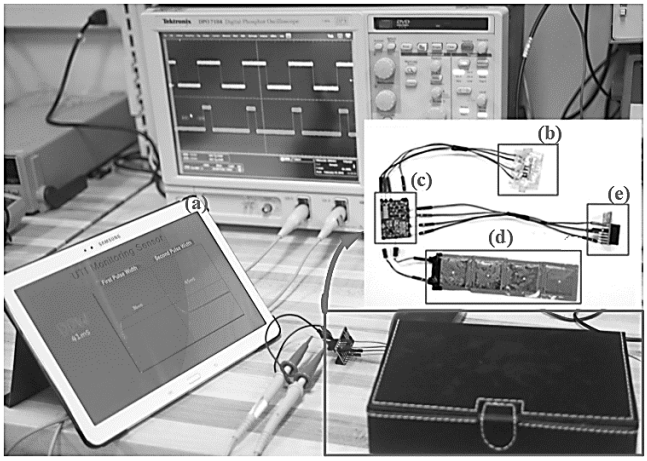

Fig. 10. A photograph of the measurement set-up.
(a) Mobile app displaying nitrite concentration in real time (b) colorimetric nitrite sensor (c) DC-DC boost converter and sensor interface (d) urine-activated battery (e) BLE module (RFD22102)

Fig. 10 shows a measurement set-up used for the experiments. The boost DC-DC converter and the PWM sensor interface are mounted on a custom printed circuit board (PCB). The sensor includes an LED with the peak emission wavelength of 572nm and two photodiodes with the peak sensitivity wavelength of 540mm. The LED bias current is set to 0.5mA, and the PWM sensor interface draws 0.08mA from the regulated 2V supply. The microcontroller in the BLE module (RFD22102 from RFDuino) provides timing signals and converters the pulse width output of the PWM sensor interface into digital data that is transmitted to a paired mobile device (nVidia tablet). The BLE module draws 4mA in transmission mode

Synthetic urine samples with nitrite concentrations of 0mg/L, 4mg/L, 6mg/L, 8mg/L, and 10mg/L are used for the measurements. To perform the tests, urine samples were dropped onto the sensors and the urine-activated batteries at the same time. Fig. 11. shows the voltage variation of the urine-activated batteries and the regulated voltage of the boost DC-DC converter.

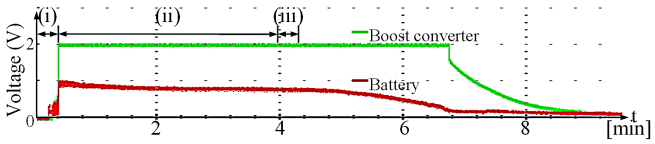

Fig. 11. Measured the battery voltage and the boost converter voltage: (i) Initial urine exposure and battery activation, (ii) DC-DC boost convert start and sensor reading (iii) BLE transmission.

The batteries are activated in 10 seconds after initial urine exposure and the boost DC-DC converter starts operation when the voltage of batteries reaches a start-up voltage of 0.5V. Then the colorimetric sensor starts reading. The PWM signals for the dry reagent strip and for the wet reagent strip were measured as shown in Fig. 12.

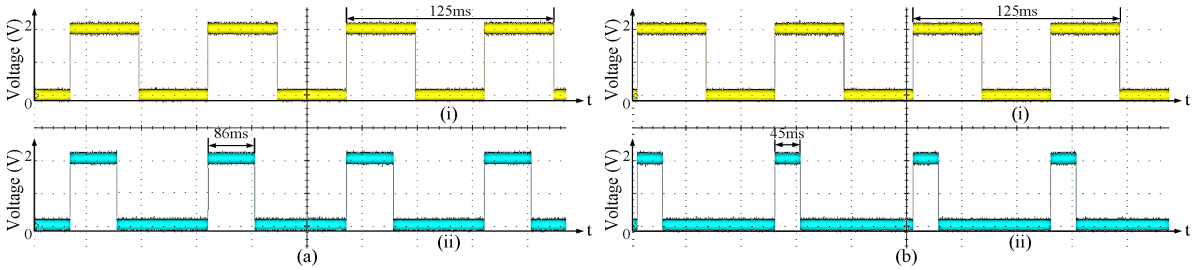

Fig. 12. Measured PWM signal (a) Pulse width for the dry reagent strip: (i) Clock signal, (ii) Output VPWM signal, and (b) Pulse with for the wet reagent strip: (i) Clock signal, (ii) Output VPWM signal.

The BLE module digitizes the PWM signals and transmits them. Fig. 13 shows T_{PW1}, T_{PW2}, and the differential pulse width displayed on the mobile device at real-time.

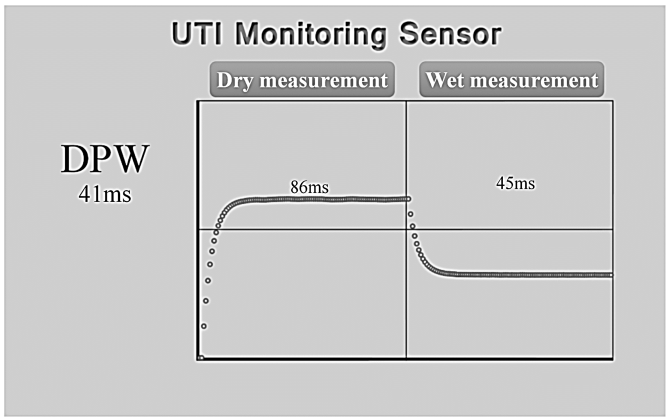

Fig. 13. Displayed result on the mobile device.

Fig. 14(a) illustrates the differential pulse width versus nitrite concentrations curves for an ideal case simulation and measurements before and after the calibration.

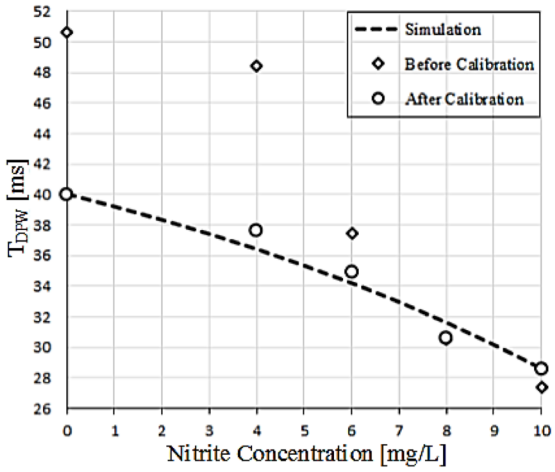

Fig. 14. (a) Measured differential pulse width versus nitrite concentrations (b) Conventional dipstick color chart.

For the measured differential pulse width T_{DPW} before the calibration, the maximum error from the ideal case simulation reaches up to 33%, while the T_{DPW} after the calibration shows a maximum error of 3.5%, which corresponds to almost 10 folds of improvement. The sensor module achieves a sensitivity of 1.35 ms/(mg/L) and a detection limit of 4 mg/L for nitrite. Because nitrite is never found naturally in urine, and many species of gram-negative bacteria convert nitrate to nitrite, the T_{DPW} of urine from a person without UTI will show 40ms. The T_{DPW} of the urine of a person with UTI will be smaller than 40ms, and the difference will increase with increasing amount of nitrite in the urine. Fig. 14 (b) shows a reference color chart of typical urine dipsticks designed for nitrite detection. To the untrained eyes, a quantitative analysis on nitrite concentration, beyond the decision on positive or negative, is not feasible for dipsticks.

Fig.15 presents the measured differential pulse width with liquid samples, showing that the differential pulse width changes by 2.03%.

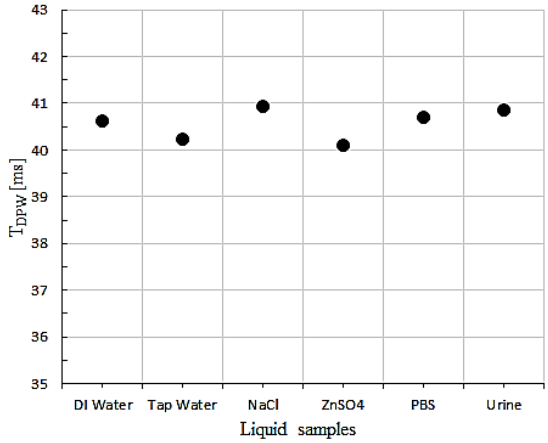

Fig. 15. Measured differential pulse width versus liquid samples.

Although the urine composition varies among patients, the sensor module should correctly detect only nitrite for UTI. In order to verify the sensor module specificity to nitrite, different types of solutions such as deionized (DI) water, tap water, NaCl of 500mg/L, ZnSO4 of 500mg/L, phosphate-buffered saline (PBS), and synthetic urine were used. These experimental results prove that the sensor module can detect nitrite reliably regardless of liquid samples.

IV. Custom Integrated Circuit (IC)

Small size and low power consumption of a sensing module is highly desirable for medical sensing applications. Reducing power and size of a sensing module is challenging particularly when the module relies on off-the-shelf commercial components. To further optimize power and size of the developed sensor module, we are developing a custom integrated circuit (IC) that includes a DC-DC converter, an LED driver, and a sensor interface in TSMC 65nm technology.

V. Future Work

In the following year, we will characterize the performances of the fabricated custom IC, and build a new prototype UTI sensing system utilizing the custom IC. We expect significant improvements in size and power efficiency. We will also conduct tests with natural human urine, instead of using synthetic urine, in collaboration with a urologist at the Indiana University Medical School.